

## RAIN-INDUCED EROSION: A STUDY IN BADLANDS NATIONAL PARK

Emily C. French<sup>1</sup>, Donna Kliche<sup>1\*</sup>, Paul Smith<sup>1</sup>, and Larry D. Stetler<sup>2</sup>

<sup>1</sup>Atmospheric Sciences Department

<sup>2</sup>Geology and Geological Engineering Department

South Dakota School of Mines and Technology

Rapid City, SD 57701

\*Corresponding author address: e-mail: Donna.Kliche@sdsmt.edu

### ABSTRACT

Factors that may influence the severity of erosion at a given location include soil composition, annual rainfall, climate, and vegetation type and coverage. This study addresses the ongoing erosion occurring in the Badlands National Park (BNP) in South Dakota. The research work is aimed to determine a better measurement of the rain erosion in the BNP using a laser optical disdrometer and erosion scales. A Parsivel disdrometer instrument was installed during May-September, 2011, to measure raindrop sizes and their fall velocities. Using these variables, we calculated the rainfall intensities and kinetic energy fluxes of individual rain events, the main parameters needed to estimate the rain induced erosion rate. Rain events were categorized as light, moderate, and heavy based on rainfall intensity, as well as either convective or stratiform based on radar data. Heavy events that also produced hail were considered an additional category. Comparisons between kinetic energy fluxes associated with hail- and non-hail producing events showed a clear separation: an average of 1574 J/m<sup>2</sup> for the 08/03/2011 hail-producing event and a range of 296 to 485 J/m<sup>2</sup> for non-hail producing events. Such a distinction could play a significant role when it comes to erosion prediction in areas which see numerous hail events annually. It should be noted that only raindrop size diameters were included in the calculations (any measured diameters > 7mm were excluded to remove hailstones from being included in calculated kinetic energy fluxes). Preliminary results also show that our estimated rain induced erosion rate is larger (7.2x10<sup>6</sup> J mm m<sup>-2</sup> hr<sup>-1</sup> yr<sup>-1</sup>) than the current interpolated value from isoerodent maps for this region (1.01x10<sup>5</sup> J mm m<sup>-2</sup> hr<sup>-1</sup> yr<sup>-1</sup>).

### Keywords

Erosion rates, disdrometer, rainfall, wet erosion

### INTRODUCTION

Water erosion is often a result of rainfall. Wischmeier and Smith (1958) estimate that the amount of water falling in 30 minutes of a typical thunderstorm in

the central United States may exceed  $25 \text{ kg/m}^2$  (100 tons/acre). Each raindrop, as it falls from the base of the cloud, has a kinetic energy associated with it given by the product of its mass and its velocity squared. The number of raindrops falling on a unit surface at the ground can be associated with a kinetic energy (KE) flux which can be large or small depending on the rain intensity associated with the rain event. Wischmeier and Smith (1958) also estimated the KE flux in a single thunderstorm to be approximately  $670 \text{ J m}^{-2}$ . These effects can be more severe if the rain is accompanied by strong winds.

The present geomorphology at Badland National Park (BNP) was caused by erosion and deposition of sediment by the wind, water, and freeze-thaw activity (BNP 2011). Erosion causes fossils to be exposed at the surface (by sediment removal) or become buried (by sediment deposition). Preservation of these fossils is essential to BNP. The estimated erosion rate for this site is about 2.5 cm (1 in) per year, indicating that many geologic formations at BNP could completely erode away in few hundred years. However, the climatic variability recorded in the last decade over the entire globe raises justifiable concerns regarding existing erosion rate estimates. Our research is aimed to provide a better measurement of the rain erosion in the BNP using a laser optical disdrometer and erosion scales. The OTT Parsivel Laser-Optical Disdrometer provides high resolution raindrop size data and raindrop velocity data which can help achieve this objective.

The ability to accurately measure rain erosion rates is also essential to areas other than the BNP. Initially, erosion and soil loss prediction algorithms were developed for agricultural use to forecast the long term average annual rate of erosion on a field slope based on rainfall pattern, soil type, topography, crop system and management practices. Over time, it has also been used in urban planning (Renard et al. 1991). The Revised Universal Soil Loss Equation (RUSLE) is a widely used method for soil erosion prediction (Renard et al. 1991). One of the parameters in this equation is the *R-factor*, which is an indicator for rainfall erosion rate. According to Wischmeier and Smith (1978) and Renard and Freimund (1994), this value is normally calculated using rain gauge data alone.

The current research involves an alternative means for *R-factor* calculation using the more relevant and time-resolved raindrop size measurements of the disdrometer. This new information will allow BNP to identify situations where erosion may be more serious than initially thought and assist them in developing strategic plans for the survey and removal of fossils before they are damaged by erosion and theft.

The Parsivel disdrometer belonging to the Department of Atmospheric Sciences at the South Dakota School of Mines and Technology (SDSM&T) allows evaluation of high-resolution rainfall data. At BNP, a cooperative erosion study between the Department of Geology and Geological Engineering, and BNP researchers was initiated in 2010. The addition of the high-resolution rainfall data to this erosion study provided additional information to better predict erosion from rainfall. The present overall erosion study carried out in BNP using the latest technology for rainfall and erosion measurement is one of the first at this location.

***RUSLE Model and the R-factor***—The erosion rate estimates are calculated using the Universal Soil Loss Equation (USLE) that was initially developed in

the late 1950's for agricultural use (Renard et al. 1991). The USLE predicts the amount of soil loss from sheet or rill erosion on a single slope, but does not account for soil losses that may occur from wind (dry erosion) or tillage erosion (from plowing fields). Revision of the USLE began in 1987 and was completed by Renard et al. (1991). The resulting RUSLE equation has the same mathematical form as the USLE, but with adjustments in calculating some of the factors:

$$A = R \times K \times LS \times C \times P, \tag{1}$$

where  $A$  is the potential long term average annual soil loss in  $\text{kg m}^{-2} \text{yr}^{-1}$  (mass/area\*year),  $R$  is the rainfall-runoff erosivity factor (from here-on we refer to it as the  $R$ -factor) in  $\text{MJ mm m}^{-2} \text{hr}^{-1} \text{yr}^{-1}$  (erosivity unit/area\*year),  $K$  is the soil-erodibility factor in  $\text{kg hr MJ}^{-1} \text{mm}^{-1}$  (mass/erosivity unit),  $LS$  is the slope length-gradient factor,  $C$  is the crop/vegetation and management factor, and  $P$  is the support practice factor. As stated by Renard et al. (1991), the four main factors affecting erosion are given and represented by these constituents: a) climate erosivity ( $R$ -factor), b) soil predisposition to erosion due to its physical and chemical structure ( $K$ ), c) topography ( $LS$ ), and d) land use and management practices ( $CP$ ). It should also be noted that  $L$ ,  $S$ ,  $C$ , and  $P$  are dimensionless, and the units of  $A$  depend only on the  $R$ -factor, and  $K$ .

Wischmeier and Smith (1978) indicate that storm soil losses due to erosion are proportional to the kinetic energy times the intensity ( $KE$ - $I$ ) of rainfall, where  $KE$  is the total storm kinetic energy in  $\text{J m}^{-2}$  (i.e. erosivity unit), and  $I$  is the maximum 30-minute rainfall intensity in  $\text{mm hr}^{-1}$ . Renard and Freimund (1994) defined the  $R$ -factor ( $R$  in the equation below) as the sum of individual storm  $KE$ - $I$  values in a year, averaged over periods greater than 20 years:

$$R = \frac{1}{n} \sum_{j=1}^n \left[ \sum_{k=1}^m \left( \frac{KE \times I_{30}}{2} \right)_k \right]_j,$$

where the total storm kinetic energy,  $KE$ , has units of  $(\text{MJ m}^{-2})$ ,  $I_{30}$  is in  $(\text{mm hr}^{-1})$ ,  $j$  is the index of number of years used to produce the average,  $n$  is the total number of years used to obtain the annual average  $R$ -factor,  $k$  is the index of the number of storms in each year, and  $m$  is the total number of storms in each year.

The  $R$ -factor values for different geographic areas are currently contained in tables originally calculated based on climatological rain gauge data. Renard and Freimund (1994) give the four steps for estimating  $R$ -factor values for areas without data by drawing isoerodent maps. Isoerodent maps connect points which have the same  $R$ -factor value (isolines). Isolines and the inferred  $R$ -factor values between isolines are only estimations because rain gauge data are sparse (Steiner and Smith, 2000). The more recent high resolution rainfall measurements, like the data from disdrometers, can be used as a new method for updating  $R$ -factor estimates.

**The Parsivel Disdrometer**—The Parsivel disdrometer shown in Figure 1 is a laser-based optical system that measures particle sizes and their respective fall velocities for several types of precipitation (Löffler-Mang and Joss 2000).



Figure 1. Ott Parsivel Laser Optical Disdrometer, 1st generation.

The laser beam is emitted from one node as a flat sheet with a horizontal cross-section area of  $0.0054 \text{ m}^2$  through which hydrometeors fall and is received on the other. The disdrometer was designed to identify 32 fall velocity classes and 32 size classes. The velocity classes range from  $0.05 \text{ m s}^{-1}$  to  $22.4 \text{ m s}^{-1}$ , while the size classes range from  $0.062 \text{ mm}$  to  $26 \text{ mm}$  in diameter. Using the size and velocity data, this disdrometer is capable of distinguishing between eight different types of hydrometeors: drizzle, drizzle with rain, rain, rain/drizzle with snow, snow, snow grains, freezing rain, and hail.

**Rainfall Kinetic Energy and Intensity Calculation**—As described in detail in French (2012), the rainfall kinetic energy fluxes for this study are derived from the raindrop diameters  $D$  obtained from the drop size distribution (DSD) measurements, and the fall velocity  $V$  measured by the disdrometer or estimated from the empirical law of Atlas et al. (1973):

$$V(D) = 9.65 - 10.3 \times \exp(-0.6D) \quad (3)$$

with  $D$  in mm and the fall speed in  $\text{m s}^{-1}$ . The time-specific rainfall kinetic energy flux [ $\text{J m}^{-2} \text{ hr}^{-1}$ ] for each raindrop sample is given by:

$$KE_{time}(DSD) = \rho_w \frac{\pi}{12} \frac{1}{A\Delta t} \sum_i n_i \times \left( \frac{1}{D_{b,i} - D_{a,i}} \times \int_{D_{a,i}}^{D_{b,i}} D_i^3 dD \right) \times \left( \frac{1}{V_{b,i} - V_{a,i}} \times \int_{V_{a,i}}^{V_{b,i}} V_i^2 dV \right), \quad (4)$$

where  $\rho_w$  is the water density (in  $\text{kg m}^{-3}$ ),  $V_i$  is the raindrop fall velocity ( $\text{m s}^{-1}$ ),  $n_i$  is the number of drops in class size  $i$ ,  $A$  is the instrument's sampling area,  $\Delta t$  is the sampling interval (in hr),  $D_i$  is the diameter of class size  $i$ , ranging from  $D_{a,i}$  to  $D_{b,i}$ . From here on, the time-specific rainfall kinetic energy flux ( $\text{J m}^{-2} \text{ hr}^{-1}$ ) calculated using the disdrometer-measured raindrop velocities is referred to as  $KE_1(DSD)$  and when calculated with raindrop velocities given by Eq. (3), is referred to as  $KE_2(DSD)$ .

The corresponding rainfall intensity  $I(DSD)$  in [ $\text{mm hr}^{-1}$ ] is calculated for each rainfall event using:

$$I(DSD) = \frac{\pi}{6} \frac{1}{A\Delta t} \sum_i n_i D_i^3 \left( \frac{1}{D_{b,i} - D_{a,i}} \times \int_{D_{a,i}}^{D_{b,i}} D_i^3 dD \right) \quad (5)$$

METHODS

The present research estimated individual storm *KE-I* values using high resolution raindrop size measurements during the summer of 2011. For this study, the disdrometer was set up to produce a drop size distribution (*DSD*) data output telegram every 10 seconds which included time, date, rainfall intensity and rainfall accumulation, total number of particles detected, and the counts and velocity for each hydrometeor size class.

**Research Site Location**—The site for this study was in the North unit of the Badlands National Park (Figure 2) where the disdrometer was placed to the southeast of the BNP visitor’s center.

The U.S. Climate Data for Interior, SD, places the annual average high temperature at 17.6 °C (63.7 °F), the annual average low temperature at 2.9 °C (37.2 °F), and the average annual precipitation at 457.2 mm (18.0 in) per year (USCD 2011). The average high and low temperatures for the months of this study (May – September) are 28.8 °C (83.8 °F) and 12.8 °C (55 °F), respectively. The hottest months (July and August) have average high temperatures of 32.8 °C (91 °F), which is slightly higher than the high temperatures experienced during this study. The average total precipitation (as of 2011) from May through September (the months of data collection) is 291.9 mm (11.49 in), with the wettest month being May at 81.0 mm (3.2 in) and the driest month being September with 31.0 mm (1.2 in).

**The Parsivel Instrument**—A solar powered Parsivel disdrometer (Figure 3) was installed in an open area near a small butte, and data were collected between May 11, 2011 and September 30, 2011. The 10-second data fields were first



Figure 2. North Unit of the BNP. INTS2 weather station is shown, as well as the Visitor’s Center. The disdrometer was placed to the southeast of the Visitor’s Center.



Figure 3. The Parsivel disdrometer and its power source, a solar panel, on location in the North Unit of the BNP.

compiled into 1-min data, followed by calculation of the 5-min data from the 5 sequential 1-min data. The 30-min data were then grouped from 6 sequential 5-min rainfall samples (French 2012). For the present analysis, only rain events lasting 15 min or more and with minimum accumulated rainfall of 6 mm were considered. This constraint was further quantified by excluding measurements with rainfall intensities less than  $0.1 \text{ mm hr}^{-1}$  (based on 1 min rainfall intensity data).

**Erosion Scale Data**—To obtain a quick measurement of the hill-slope erosion that took place in 2011, we installed erosion scales in early May and read them to the nearest 0.5 mm (Figure 4). The scales were installed in bedrock on opposite sides of a butte nearby the disdrometer: one side of the butte sloped downward at an angle of 28 degrees and faced to the North, while the opposite side sloped downward at an angle of 33 degrees and faced to the South. The South-facing slope had erosion scales at the top and at the middle of the slope. The North-facing slope had erosion scales at the top, the middle, and at the bottom of the slope.



Figure 4. One of 5 erosion scales placed on a North- and South-facing slope on a butte near Parsivel disdrometer.

Initially, direct erosion measurements were planned to be taken after each rain event to quantify the amounts of erosion produced. However, transportation to the site after each event proved to be difficult due to the high frequency of such rainfall events during summer 2011. As described in French (2012), the sediment levels at erosion scales were collected on only six different occasions between May 5, 2011 and October 10, 2011. These values are provided in French (2012) and will be used for the on-going research at BNP site to estimate the long term annual soil loss (Eq. 1).

**Tipping Bucket Rain Gauge**—On the corner of the solar panel stand, a tipping bucket rain gauge was installed (Figure 5) to measure rainfall intensities and depths. Rain was collected in a small bucket of known depth (0.254 mm or 0.01 in). When this amount was exceeded, the bucket tipped over releasing the water. The number of tips was recorded by an internal data logger. The number of bucket tips in a time interval determines the rainfall intensity. The number of bucket tips multiplied by the tipping bucket rainfall depth yields rainfall accumulation.

However, much of the rain gauge data of rainfall depth and intensity were not comparable to either the disdrometer or the neighboring weather observing platforms measurements. We determined that the rain gauge data were too corrupt to be used in this study. One possible explanation can be a hail event early in the sampling period which could have damaged the instrument internally and affected subsequent measurements. The presence of hail and heavy rain intensities throughout the sampling period (summer 2011) may have caused amplified data contamination. We hope that a continuation of this study can be completed with a rain gauge which will accurately estimate rainfall rates and accumulations.



Figure 5. Tipping bucket rain gauge attached to the Solar Panel.

**Weather Observing Platforms**—Disdrometer rainfall data were compared to weather data collected at four neighboring locations. An aerial photograph of these locations is in Figure 6 (from Google Maps). The site closest to the disdrometer is the INTS2 National Weather Service (NWS) observation site in Interior, SD. The next closest site is the Mesowest **Remote Automatic Weather Station**, which will be referred to as PINS2. This site is located just south of Interstate 90 at the North entrance to the BNP.

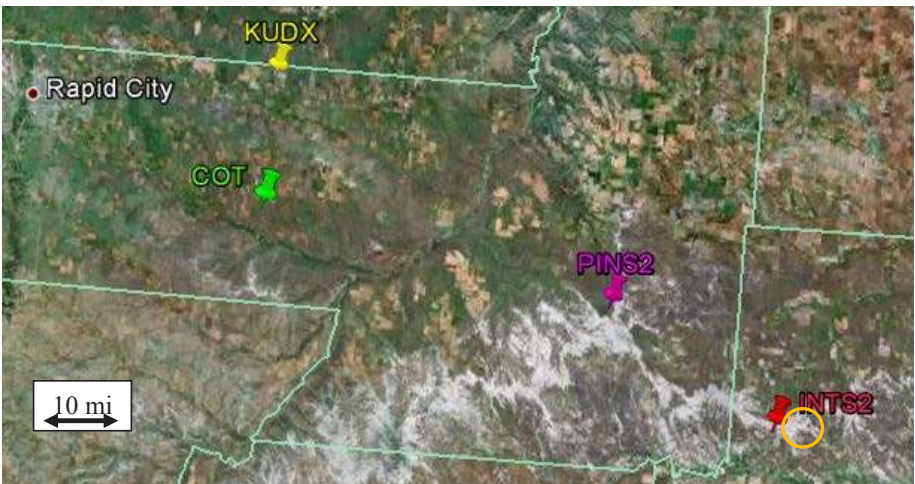


Figure 6. Aerial view of the weather data recording sites utilized in this study, INTS2, PINS2, COT, and KUDX. The location of the disdrometer is noted by the orange circle.

The Automated Weather Data Network site at Cottonwood (COT) is the surface weather station at the farthest distance from the study site. More details on these sites can be found in French (2012).

Each rainfall event was classified as light, moderate or heavy based on rainfall intensity using the 1-min data (Table 1). After storm intensity was determined, rain events which were either moderate or heavy were subjectively classified as convective or stratiform type. This delineation was determined by rain intensities and durations, as well as the overall synoptic meteorological setup of each event. Radar reflectivity data (from KUDX) were also utilized to characterize convective vs. stratiform precipitation.

**Table 1. Rainfall event classification based on intensity of both the Parsivel's manual and the NWS standards. \*A small sampling of light events and the difficulty detecting such low intensities caused this value to be increased for this study to intensities averaging around 0.3 mm hr<sup>-1</sup>.**

Rainfall Event Intensity	Parsivel Intensity Range (mm hr <sup>-1</sup> )	NWS Intensity Range (mm hr <sup>-1</sup> )
Light	≤ 0.2*	≤ 0.2
Moderate	0.2 – 4.0	0.5 – 7.5
Heavy	> 4.0	> 7.5

The rain events which coincided with widespread precipitation with lower to moderate radar reflectivities (approximately <55 dBZ) were considered stratiform events. An example of such an event is given in Figure 7. Contrastingly, radar reflectivities which clearly showed individual storm cells or a line of storm cells with high radar reflectivities (approximately >55 dBZ) were considered convective events (Figure 8). In most cases, these events were shorter-lived than stratiform events.



**Figure 7. KUDX radar reflectivity data for a stratiform event which passed over Parsivel location on 7/11/2011.**

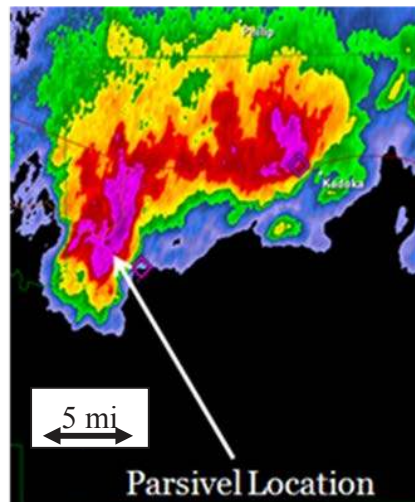


**Figure 8. KUDX radar reflectivity data for a convective event which passed over Parsivel location on 9/3/2011.**



For each of the rain events chosen for this study, weather data from INTS2, PINS2, and COT were examined. For events where hail was reported at INTS2 or particles >7 mm were measured by the disdrometer, radar data from KUDX were consulted. Radar data were also examined for all moderate events to delineate between convective and stratiform type events.

**KE-I and the R-Factor Calculation**—The equations shown earlier were used to calculate *KE* fluxes and rainfall intensity *I* values. For a selected light event, and a selected moderate event, each 30-minute accumulation (mm) as given by the disdrometer was determined. Each 30-minute accumulation (mm) was multiplied by the corresponding 30-min average *KE* ( $J\ m^{-2}\ mm^{-1}$ ), which yields the average 30-minute kinetic energy ( $J\ m^{-2}$ ). The sum of all of the average 30-minute kinetic energies through the storm lifetime gives the total storm kinetic energy ( $J\ m^{-2}$ ). This value is then multiplied by the maximum 30-minute intensity ( $mm\ hr^{-1}$ ) for the storm ( $I_{30}$ ). This value of the *KE-I* ( $J\ mm\ m^{-2}\ hr^{-1}$ ) is proportional to the erosion produced by a particular storm. These calculations were performed for both  $KE_1(DSD)$  and  $KE_2(DSD)$  cases (see Eqs.4 and 5). The average of these values over a number of years (20 or more years) then provides the average rain induced erosion rate per year, i.e., the *R-factor* used in the *RUSLE* equation.

## RESULTS AND DISCUSSION

For all light, moderate, and heavy events identified for this study, the  $KE_1(DSD)$ ,  $KE_2(DSD)$ , and  $I(DSD)$  for 1-min and 30-min rainfall data were calculated. A representative event for each rainfall intensity type was chosen for in-depth analysis, and the corresponding storm erosion rate (*KE-I*) value was estimated.

Table 2 contains a summary of the sampled events based on storm type. More information on the dates for specific events is provided in French (2012).

**Table 2. Summary of rain events from May through September 30, 2011.**

Rainfall Event Intensity	Number of Events	Average Intensity (Parsivel) (mm/br)	Average Intensity (Calculated) (mm/br)	Stratiform/Convective (S/C)	Total Duration (hr)
Light	3	0.3	0.3	3S	7:05
Moderate	20	1.9	1.9	18S/2C	17:56
Heavy	6	6.6	5.8	1S/5C*	6:31
Hail	11	28.1	55.7	11C	12:12

\*One heavy-intensity storm transitioned from convective to stratiform while it passed over the disdrometer’s location, and was counted once in the convective event category.

**Light Rainfall Events**—The three light intensity events considered for this study were of stratiform type and had durations of 5.02 hours, 1.58 hours, and

0.48 hours. Additionally, the observed average rainfall intensities were in the range of 0.28 to 0.33 mm hr<sup>-1</sup>, which is borderline with the moderate type intensity when considering Parsivel's classification of events based on rainfall intensity.

Figure 9 presents the  $KE_1(DSD)-I(DSD)$  and  $KE_2(DSD)-I(DSD)$  relationships based on 1-min data for all of the light intensity events. The  $KE-I$  relationships for the light events were the simplest to analyze because there was no hail and no convective activity.

The longest-duration event, May 11, 2011 from 17:52 MDT to 22:53 MDT, had an average storm intensity of 0.306 mm hr<sup>-1</sup> as given in the telegram by the disdrometer. Using calculated 1-min intensities (Eq. 5), we determined the average kinetic energy flux  $KE_2$  for this event to be 34.59 J m<sup>-2</sup> hr<sup>-1</sup> (Eq. 4). This  $KE_2$  is only 20% of the  $KE_1$  (178.35 J m<sup>-2</sup> hr<sup>-1</sup>) which uses the disdrometer measurements of the raindrop fall velocities. Since  $KE_1$  values seemed much larger than  $KE_2$  (which uses Eq. 3 to calculate velocity), we performed a more detailed investigation of the disdrometer data [see French (2012) for details]. The results of the additional tests on the data suggest that the disdrometer was overestimating the fall velocities of raindrops at low rainfall intensities, a fact admitted by the manufacturer and corrected for the 2<sup>nd</sup> generation of Parsivel instruments. INTS2 reported a trace amount of precipitation for the 24-hour period that included this event, while the disdrometer reported a total accumulation of 1.34 mm.

**Moderate Rainfall Events**—The 20 moderate events observed ranged in duration from 0:12 hours to 16:08 hours. These events were mostly of the stratiform

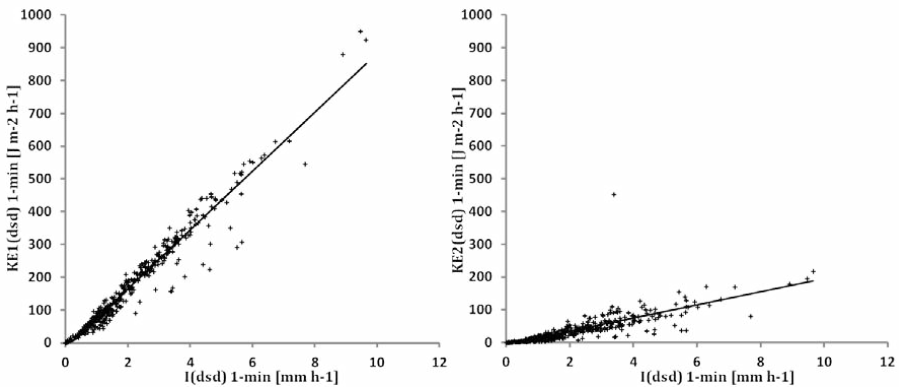


**Figure 9.**  $KE_1(DSD)-I(DSD)$  and  $KE_2(DSD)-I(DSD)$  1-min data relationships for light events occurring between May and September 30, 2011. The graph on the left uses  $KE_1$ , and the graph on the right uses  $KE_2$ . Linear fits are provided to show the qualitative spread in data points.

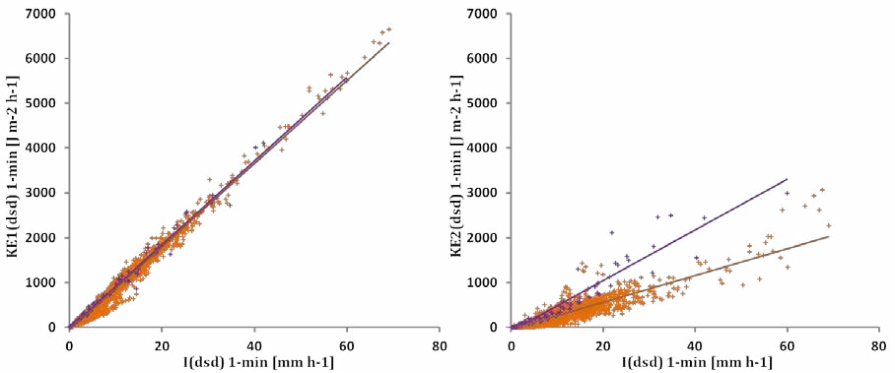
type, while two of the events did appear convective in nature based on radar reflectivity observations and were classified as such. These two convective events had the highest rainfall intensities for the moderate range type.

Figure 10 presents the  $KE_1(DSD)-I(DSD)$  and  $KE_2(DSD)-I(DSD)$  relationships based on 1-min data for the moderate intensity events. In the case of 1-min data, events were also separated between convective and stratiform types.

Convective events are denoted by purple colors, and stratiform events are in orange. The  $KE-I$  relationship for moderate events does not seem to be different between moderate convective and moderate stratiform events in the case of  $KE_1$ . However, the difference between  $KE-I$  relationships for convective and stratiform events is visible when  $KE_2$  is used. Also, when the range of values between  $KE_1$  and  $KE_2$  are compared, we see that the  $KE_2$  range is about half of the corresponding range values for  $KE_1$ . This finding is again a confirmation of the initial findings of possible glitches in raindrop velocity measurements by 1<sup>st</sup> generation of Parsivel disdrometers. These issues were corrected for the 2<sup>nd</sup> generation.

The event which occurred on June 19, 2011 was a good example of a moderate intensity stratiform type event. It lasted from 23:11 MDT to 1:37 MDT on June 20, 2011, for a total duration of 2 hours and 36 minutes. The event had an average  $KE_1$  of  $981 \text{ J m}^{-2} \text{ hr}^{-1}$ , while  $KE_2$  yielded an average of  $358 \text{ J m}^{-2} \text{ hr}^{-1}$ .

**Heavy Rainfall Events**—A total of 17 heavy rainfall events were examined ranging in duration from 0:13 hours to 2:51 hours. Figure 11 presents the  $KE_1(DSD)-I(DSD)$  and  $KE_2(DSD)-I(DSD)$  relationships based on 1-min data



**Figure 10.**  $KE_1(DSD)-I(DSD)$  and  $KE_2(DSD)-I(DSD)$  1-min data relationships for moderate events occurring between May and September 30, 2011. The graph on the left uses  $KE_1$ , and the graph on the right uses  $KE_2$ . Note that x-,y-axis range are different than in Figure 9. Convective events are in purple and stratiform events in orange.

for all 17 of the heavy intensity events. Events were separated between hail and non-hail producing type, where hail events are denoted by blue color and non-hail events are in pink. Note the similarity of range values between  $KE_1$  and  $KE_2$ , an observation not made in the case of light and moderate rainfall events. Remarkable, however, is the difference in  $KE-I$  range values between hail and non-hail events (for both  $KE_1$  and  $KE_2$ ) although no particle  $>7$  mm (hailstones) was included in the  $KE-I$  calculations.

A detailed description of some specific heavy rainfall events and their characteristics is given in French (2012).

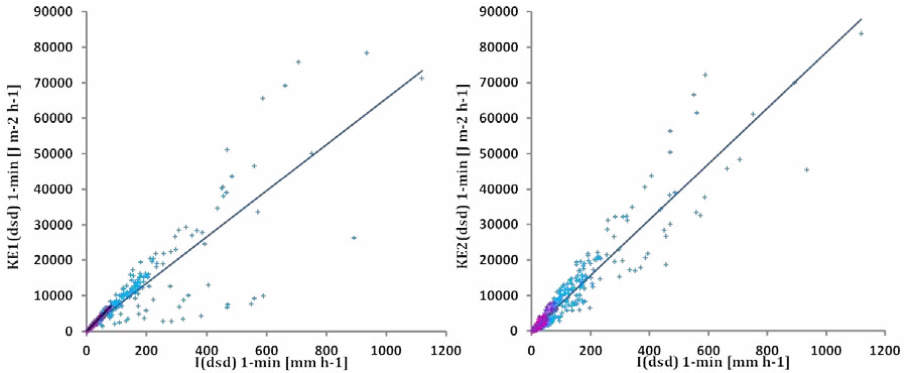


**Figure 11.**  $KE_1(DSD)-I(DSD)$  and  $KE_2(DSD)-I(DSD)$  1-min relationships for all heavy events occurring between May and September 30, 2011. The graph on the left uses  $KE_1$ , and the graph on the right uses  $KE_2$ . Note that x-,y-axis range are different than in Fig. 9 or Fig. 10. Hail events are in blue and non-hail producing events are in pink.

One of the most interesting event occurred on August 3, 2011, between 18:37 MDT and 20:51 MDT. The average  $KE_1$  for this event was  $3734 \text{ J m}^{-2} \text{ hr}^{-1}$ , while the average  $KE_2$  was  $4005 \text{ J m}^{-2} \text{ hr}^{-1}$ . Interestingly, this event showed the first occurrence of  $KE_2$  larger than  $KE_1$ , by only about 7%. The disdrometer indicated that the largest recorded particles were sampled between 23 mm and 26 mm (class 32), which is the maximum size it can detect. This is equivalent to approximately 1-inch hail. At 18:47 MDT the most hydrometeors per minute were detected for the entire event (4030 total counts). Interestingly, it was during this minute when the most hail counts per minute (=201) were measured. In addition, the rainfall intensity was so high that the disdrometer was unable to measure the rain accumulation for that minute.

***KE-I and R-factor Results***—Four events, each being representative for the rainfall intensity category, were selected to calculate corresponding  $KE-I$  values: light intensity, moderate intensity, heavy intensity, and heavy intensity with hail. The  $KE-I$  values were estimated using  $I_{30}$ ,  $KE_1$  and  $KE_2$  as explained earlier. Table 3 provides the storm duration, intensity, precipitation type, and the maximum 30-minute intensity, while Table 4 includes the rainfall amounts, calculated  $KE_1$  and  $KE_2$ , as well as the corresponding total  $KE-I$  values for the selected events shown in Table 3.

**Table 3.** Representative events details for each intensity classification (light, moderate, heavy, and heavy-hail). Each event is also categorized as convective (C) or stratiform (S).

Event Date	Start Time	End Time	Duration	Avg Storm Intensity	Avg Storm Intensity	Hail?	Intensity	Storm Type	Event $I_{30}$
M/DD/YY	MDT	MDT	hr	mm hr <sup>-1</sup> (Parsivel)	mm hr <sup>-1</sup> (calc)	Y/N	L/M/H/HH	C/S	mm hr <sup>-1</sup>
5/11/11	17:52	22:53	5.02	0.31	0.29	N	L	S	9.65
6/19/11	23:11	1:37	1.58	2.63	2.43	N	M	S	30.94
7/28/11	3:34	4:21	0.48	7.07	7.18	N	H	C	81.30
8/3/11	18:37	20:51	2.23	13.01	66.73	Y	HH	C	548.57

**Table 4. For the storm events in Table 3, the results for the rainfall accumulation,  $KE_1$ ,  $KE_2$ , and the corresponding total storm  $KE-I$  values are shown.**

Event Date	Rainfall Amount	$KE_1$	$KE_2$	Total Storm $KE-I$ ( $KE_1$ )	Total Storm $KE-I$ ( $KE_2$ )
M/DD/YY	mm	J m <sup>-2</sup>	J m <sup>-2</sup>	J mm m <sup>-2</sup> hr <sup>-1</sup>	J mm m <sup>-2</sup> hr <sup>-1</sup>
5/11/11	1.24	114.1	21.0	1.1 x 10 <sup>3</sup>	2.1 x 10 <sup>2</sup>
6/19/11	27.26	2398.3	768.1	7.4 x 10 <sup>4</sup>	2.4 x 10 <sup>4</sup>
7/28/11	6.21	485.3	296.3	4.0 x 10 <sup>4</sup>	2.4 x 10 <sup>4</sup>
8/3/11	29.51	2173.3	1573.5	1.2 x 10 <sup>6</sup>	8.6 x 10 <sup>5</sup>

Figure 12 presents the relationship between kinetic energy flux ( $KE_1$  and  $KE_2$ ) and the estimated  $KE-I$  value for each event, based on the data from Table 4. As shown in Figure 12, the hail-producing rainfall events show significantly larger  $KE$  flux values than non-hail producing heavy rainfall events. Again, these findings were based only on the raindrop diameters <7 mm recorded during these events and not including the hail. Of interest is also the result showing that the moderate and heavy no-hail cases are providing a similar behavior in the  $KE-I$  estimate. However, the discrepancy in the  $KE$  flux values is attributed to the difference in the duration between the moderate and heavy events (French, 2012).

The current *R-factor* value for Interior, SD, as approximated using an isoerodent map (Renard et al. 1997), is 101,125 J mm m<sup>-2</sup> hr<sup>-1</sup> yr<sup>-1</sup> (55 (hundred foot tons) in acre<sup>-1</sup> hr<sup>-1</sup> yr<sup>-1</sup>). For the present study, a simple method for estimating an annual *R-factor* value using the four selected rain events was completed. An adjustment factor was calculated for each event, assuming each event is strongly representative for its intensity class, and that the 40 events used in this study are representative of an entire year of precipitation. A ratio of the individual event accumulation over the total accumulation for the intensity class for events analyzed in this study was used as the adjustment factor. The adjustment factor was multiplied by the  $KE_1-I$  and  $KE_2-I$  values. A summation of these four values, one from each intensity class (the definition of the *R-factor*) gives a rough estimate of a 1-year (2011) *R-factor*. Table 5 shows our findings.

**Table 5. Comparison of the actual *R-factor* for the study location, to estimated value from Renard et al. (1997).**

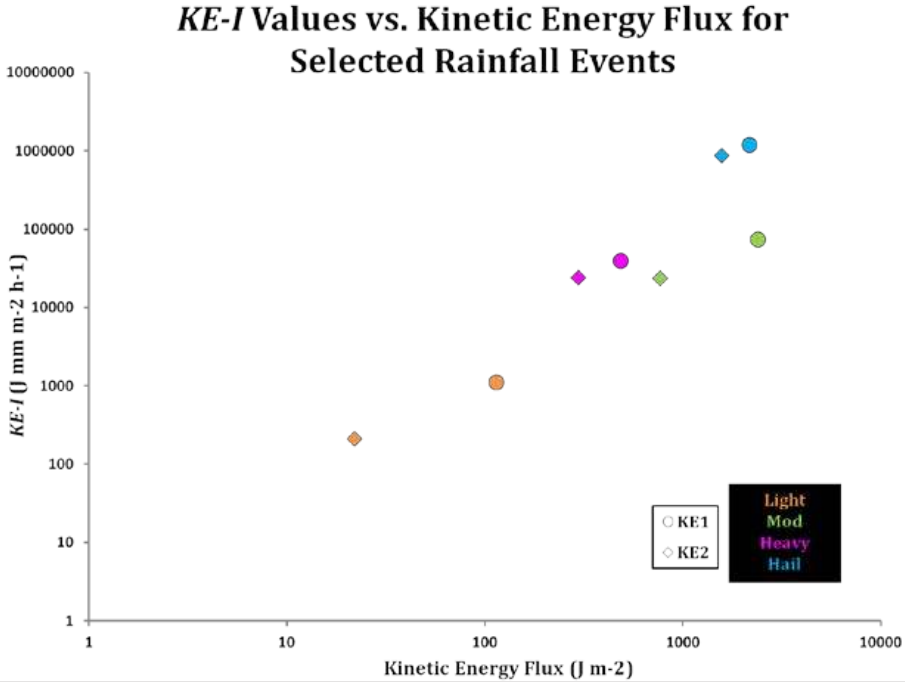


Figure 12. *KE-I* calculations based on  $KE_1$  and  $KE_2$  for selected light, moderate, heavy, and hail events from May through September 2011. Circles represent  $KE_1$  values, and diamonds represent  $KE_2$  values. Orange colors are for light events, green for moderate, pink for heavy (no hail), and blue for heavy (hail-producing). These data are from Table 4.

Adjusted Annual R-factor ( $KE_1$ )	Adjusted Annual R-factor ( $KE_2$ )	Interpolated R-factor for Interior, SD
$J\ mm\ m^{-2}\ hr^{-1}\ yr^{-1}$	$J\ mm\ m^{-2}\ hr^{-1}\ yr^{-1}$	$J\ mm\ m^{-2}\ hr^{-1}\ yr^{-1}$
$9.9 \times 10^6$	$7.2 \times 10^6$	$1.01 \times 10^5$

### CONCLUSIONS

Plots of the  $KE_1(DSD)-I(DSD)$  relationships and the  $KE_2(DSD)-I(DSD)$  relationships for light, moderate, and heavy rainfall events showed many differences, especially when it came to heavy events producing hail or not. Even after hail was removed from  $KE$  calculations, the erosive nature of the rain from hail-producing storms was far greater than the moderate and heavy intensity storms which did not produce hail. This result stresses that  $KE(DSD)-I(DSD)$  relationships should be calculated based on different rainfall intensity classifications; a single overall relationship may not suffice.

Raindrop fall velocities measured by the disdrometer generally yielded higher kinetic energy flux values ( $KE_1$ ) as opposed to when Eq. 3 is used to calculate

raindrop fall velocities based on raindrop diameter ( $KE_2$ ). Further investigation into the disdrometer data proved that the 1<sup>st</sup> generation Parsivel disdrometer overestimated the raindrop fall velocities for the light and moderate rain events. This glitch was fixed for the 2nd generation of Parsivel instruments.

The *R-factor* used in the RUSLE model has never been assumed to be the same for different geographical locations. It is indicated in the *KE-I* calculations that the *R-factor* for moderate and heavy events without hail tend to reach a maximum, and that the *KE-I* value for the two types of events is nearly indistinguishable for  $KE_1$ . The heavy event which produced hail had a noticeably higher *KE-I* value for both  $KE_1$  and  $KE_2$  as compared to the events which did not produce hail. This result suggested that the raindrop sizes and fall velocities in the hail-producing event were different enough so that the calculated *KE-I* value was significantly larger than in the case of non-hail producing events. A calculated one-year estimate of the annual *R-factor* was presented based on event-based *KE-I* values. These *R-factor* values were much greater than the *R-factor* interpolated from existing isocrodot maps for the region of interest. This is to be expected since the interpolated *R-factor* is based on 20-year average rainfall data, while our estimation is based on the summer 2011 data alone.

The results show that hail-producing events were the greatest contributor to the estimated *R-factor*. It is important to notice that our results show a clear separation of the *KE-I* values between hail and non-hail producing events, although only raindrop size diameters were included in the calculations (any measured diameters > 7mm were excluded to remove hailstones from being included in calculated kinetic energy fluxes). Such a distinction could play a significant role when it comes to erosion prediction in areas which see numerous hail events annually.

Future work will entail utilizing time-resolved rain gauge intensity data in addition to the high resolution disdrometer-measured rainfall intensity data. A better sampling of both light intensity and moderate convective-type events will be needed to validate data integrity. In addition, several years of data are needed in order to calculate averages of *KE-I* values so that a comparison with the current value for the region can be accomplished. For completeness, the comparison to observed erosion rates will also be included.

#### ACKNOWLEDGEMENTS

This research work was supported by funds from the NASA South Dakota Space Grant Consortium and the State of South Dakota. Dr. Rachel Benton, paleontologist at the Badlands National Park (BNP), helped in finding the best location for the disdrometer instrument and encouraged the efforts of this research. The erosion measurements during summer 2011 were done by Dr. Larry Stetler, professor in the Department of Geology and Geological Engineering at South Dakota School of Mines and Technology, who frequently advised during this research project.

#### LITERATURE CITED

- Atlas, D., R.C. Srivastava, and R.S. Sekhon. 1973. Doppler radar characteristics of precipitation at vertical incidence. *Rev. Geophys. Space Phys.* 11: 1-35.
- BNP. 2011. Badlands National Park. Available at <http://www.nps.gov/badll/index.htm> [Cited in 2011].
- French, E.C. 2012. An Investigation into Rainfall Kinetic Energy for Estimation of the Rainfall-Runoff Erosivity Factor, R, Using an Optical Disdrometer. MS Thesis, South Dakota School of Mines and Technology, Rapid City, SD. 108pp.
- Löffler-Mang, M., and J. Joss. 2000. An optical disdrometer for measuring size and velocity of hydrometeors. *Journal of Atmospheric and Oceanic Technology* 17: 130-139.
- Renard, K.G., and J.R. Freimund, 1994. Using monthly precipitation data to estimate the *R-factor* in the revised USLE. *Journal of Hydrology* 157: 287-306.
- Renard, K.G., G.R. Foster, G.A. Weesier, and J.P. Porter. 1991. RUSLE – Revised Universal Soil Loss Equation. *Journal of Soil and Water Conservation* 46 (1), 30-33.
- Renard, K. G., G. R. Foster, G. A. Weesier, D. K. McCool, and D. C. Yoder, 1997. Predicting Soil Erosion by Water: A Guide to Conservation Planning With the Revised Soil Loss Equation (RUSLE), U.S. Department of Agriculture, Agriculture Handbook 703 USDA, Washington, DC, 404 pp.
- Steiner, M. and J.A. Smith. 2000. Reflectivity, rainfall rates and kinetic energy flux relationships based on raindrop spectra. *Journal of Applied Meteorology* 39: (11), 1923-1940.
- Wischmeier, W.H., and D.D. Smith 1958 Rainfall energy and its relationship to soil loss *Transactions of the American Geophysical Union* 39: 285-291.
- Wischmeier, W.H., and D.D. Smith. 1978. Predicting Rainfall Erosion Losses – A Guide to Agricultural Planning. U.S. Department of Agriculture, Agriculture Handbook 537, Science and Education Administration, USDA, Washington, DC, 58 p.